*Geophysical Research Letters*

Supporting Information for

# Microplastic Deposition and its Response to Extreme Flood Events: A Case Study of Yangtze Estuary, China

Hongyu Chen [1,2], Yu Cheng [1,4], Ying Wang [1,2], Yongcheng Ding [1,2], Chenglong Wang [1,2,3], Xuguang Feng [1,5], Qinya Fan [1,2], Feng Yuan [1,2], Guanghe Fu [1,2], Xinqing Zou [1,2,3,*]

[1] School of Geographic and Oceanographic Sciences, Nanjing University, Nanjing 210093, China

[2] Ministry of Education Key Laboratory for Coast and Island Development, Nanjing University, Nanjing 210093, China

[3] Collaborative Innovation Center of South China Sea Studies, Nanjing University, Nanjing 210093, China

[4] Geological Survey of Jiangsu Province, Nanjing, 210018, China

[5] Laboratory for Marine Geology, Qingdao National Laboratory for Marine Science and Technology, Qingdao 266061, China

Corresponding author: Xinqing Zou (zouxq@nju.edu.cn)

## Contents of this file

Text S1 to S4

Figures S1 to S4

Tables S1

## Additional Supporting Information (Files uploaded separately)

Captions for Datasets S1 to S2

## Introduction

The supplementary information provided here was to supplement the article's information and assist readers in understanding our research. Text S1 introduced the natural and economic characteristics of the study area, the Yangtze Estuary and Yangtze River. Text S2-S4 provided the detailed analytical procedure in this study. Figure S1 showed the location of the sampling core. Figure S2 displayed the excess $^{210}$Pb-depth relationship of CCYY1. Fig S3 showed the overview of microplastic characteristics in CCYY1, and Fig S4 showed the vertical distribution of microplastic abundance, diversity and sediment grain size. Table S1 compared the microplastic abundance of surface sediment with other research in Yangtze Estuary.

**Text S1. Study Area**

The Yangtze Estuary, the estuary of the main stream of the Yangtze River, is in the Middle–Lower Yangtze Plain and flows into the East China Sea. The tidal current in this area is dominated by regular semidiurnal tides. Chongming Island divides the Yangtze Estuary into the North Branch and South Branch (Fig. 1). The North Branch has historically been the main channel of the Yangtze River; however, its diversion ratio has been markedly declining since 1958, and recently, this ratio has decreased by 2–3% (J. Li et al., 2019). Covering an area of $1.8 \times 10^6$ $km^2$, the Yangtze River has a water discharge of 900 $km^3$/year (globally ranking fifth) and a sediment discharge of 480 million tonnes/year (globally ranking fourth) (Milliman & Farnsworth, 2013). Owing to the enormous sediment supply, a wide tidal flat exists near the Yangtze Estuary (Wang et al., 2017). Driven by the monsoon climate, water and sediment transport is more concentrated during the flood season (May to October), occasionally causing extreme floods (Zhao et al., 2015). The main stream of the Yangtze River flows through 11 provinces of China, some of which include the Yangtze River Delta, the earliest industrialised and most developed area of China. The production of primary form plastics in these 11 provinces reached 25.19 Mt in 2019, accounting for 25.8% of the total plastic production in China (National Bureau of Statistics of China, https://data.stats.gov.cn/easyquery.htm?cn=E0103).

**Text S2. Procedures of microplastic analysis**

Pretreatment and identification. Samples weighing 20–30 g (dry weight, dw) were placed in a 500-mL glass beaker. The heavy liquid was then used to float the microplastics three times. Subsequently, 300 mL of saturated sodium chloride (ρ:1.2 g·cm–3) was added into the beaker for the first and second time, and saturated potassium iodide (ρ:1.66 g·cm–3) was added for the third time to improve the recovery rate. The turbid liquid was stirred for at least 1 min, and after 6 h, the supernatant was filtered through a filter membrane with a pore size of 20 μm. Finally, the filter membrane was air-dried before microscopic observation. The collected particles were analysed using a stereomicroscope (Leica, MC190, Germany) connected to a camera and image analysis

software (LAS V4.12, Germany) to measure and record length (longest axis), shape, and colour. All the suspected microplastic particles were selected according to the criteria proposed by Nor and Obbard (2014). The selected particles were analysed using micro-Fourier transformed infrared spectroscopy (μ-FT-IR, Thermo Nicolet iN 10, Thermo Fisher, USA) in transmission mode to determine the polymer type. The obtained spectrum of selected particles was compared with the standard plastic spectrum in the reference polymer spectral library, and samples with a matching rate >70% were accepted as microplastics.

Quality Control. Measures were undertaken to minimise potential microplastic contamination in the experimental processes. All the glass beakers and equipment were ultrasonicated and carefully rinsed three times in Milli-Q water before use. The saturated solution used in the experiment was first filtered through a 20-μm filter membrane. The equipment was covered with aluminium foil when not in use, and the operators wore cotton laboratory coats during the experiment. Laboratory blanks were analysed to estimate the background contamination in the process of microplastic extraction and identification, and the blank result (4.286 n/layer) was removed from the final microplastic statistical results. We excluded white fragments similar to PVC debris caused by core splitting to avoid pollution as much as possible.

**Text S3. $^{210}$Pb dating method**

The specific activity of $^{210}$Pb was obtained at 46.5 keV, and $^{226}$Ra was measured at 351.9 keV emitted by its daughter isotope $^{214}$Pb by direct gamma spectrometry (Wan et al., 1987). The activity of $^{210}Pb_{ex}$ (unsupported $^{210}$Pb) was calculated by subtracting the activity of $^{226}$Ra from the total activity of $^{210}$Pb. Radiometric $^{210}$Pb dates were calculated using a constant initial concentration dating model (CIC) (Appleby, 2002). The model can be expressed as follows:

$$N_H = N_0 e^{-\lambda t}$$

where $t$ is the age in years at depth H, λ is the decay constant for $^{210}$Pb (0.031/a), $N_0$ is the activity of $^{210}Pb_{ex}$ at the surface sediment (Bq/kg), and $N_H$ is the activity of $^{210}Pb_{ex}$ at depth H.

**Text S4. Statistical analyses**

**Correlation between microplastic abundance and plastic production**. Statistical analyses were performed using IBM SPSS Statistics, version 19 (IBM, USA). The variables were tested for normality using the Shapiro–Wilk test and the Kolmogorov–Smirnov test to determine whether to select a parametric or non-parametric analysis. Moreover, the Spearman correlation analysis, a non-parametric method, was applied to analyse the relationships between plastic production parameters, sediment grain size, and microplastic abundance. Statistical significance was set at $p<0.05$. The plastic production data of China and the Yangtze River basin were collected from the study by F. Wang et al. (2018) (1951–2000) and the National Bureau of Statistics of China (https://data.stats.gov.cn/easyquery.htm?cn=C01, 2001–2019). Plastic production in the Yangtze River basin was estimated by totalling the annual plastic production of the 11 provinces along the main stream of the Yangtze River, including Qinghai, Tibet (no data), Sichuan, Yunnan, Chongqing, Hubei, Hunan, Jiangxi, Anhui, Jiangsu, and Shanghai. Global plastic production data were obtained from Plastics Europe (https://www.plasticseurope.org/en/resources/market-data).

**Calculation of microplastic diversity.** Microplastic diversity was calculated based on the Simpson's diversity index (D) proposed by Simpson (1949), which was first used to judge the species diversity of an ecological community. The following formula was used:

$$D = 1 - \sum_{i=1}^{S} \left(\frac{n_i}{N}\right)^2,$$

where $i$ represents the type of microplastics, $n_i$ is the amount of the $i$-th microplastic, N is the total number of microplastics, and S is the quantity of microplastic types (T. Wang et al., 2018).

**Introduction of wavelet analysis.** Wavelet analysis is a widely used method for evaluating localised variations in power within a time series (Torrence & Compo, 1998), particularly in earth science, such as the cycle of the El Nino-Southern Oscillation (Torrence & Webster, 1999) and glacial and interglacial periods (Debret et al., 2007).

The period of microplastic abundance was measured using Software Past 4.03 in wavelet analysis (Hammer et al., 2001).

**References**


Debret, M., Bout-Roumazeilles, V., Grousset, F., Desmet, M., McManus, J. F., Massei, N., et al. (2007). The origin of the 1500-year climate cycles in holocene north-atlantic records. *Climate of the Past, 3*(4), 569-575. https://doi.org/10.5194/cp-3-569-2007

Hammer, Ø., Harper, D. A. T., & Ryan, P. D. (2001). Past: Paleontological statistics software package for education and data analysis. *Palaeontologia Electronica, 4*(1), 1-9. http://palaeo-electronica.org/2001_1/past/issue1_01.htm

Li, J., Jiang, C., Liu, Q., & Zhao, J. (2019). *Water and sediment discharge and riverbed evolution in the Yangtze Estuary*. Beijing: The Science Publishing Company.

Milliman, J. D., & Farnsworth, K. L. (2013). *River discharge to the coastal ocean: a global synthesis*. New York: Cambridge University Press.

Nor, N. H. M., & Obbard, J. P. (2014). Microplastics in Singapore's coastal mangrove ecosystems. *Marine Pollution Bulletin, 79*(1-2), 278-283. https://doi.org/10.1016/j.marpolbul.2013.11.025

Simpson, E. H. (1949). Measurement of Diversity. *Nature, 163*(4148), 688-688. https://doi.org/10.1038/163688a0

Torrence, C., & Compo, G. P. (1998). A Practical Guide to Wavelet Analysis. *Bulletin of the American Meteorological Society, 79*(1), 61-78. https://doi.org/10.1175/1520-0477(1998)079<0061:APGTWA>2.0.CO;2

Torrence, C., & Webster, P. J. (1999). Interdecadal changes in the ENSO-monsoon system. *Journal of Climate, 12*(8 PART 2), 2679-2690. https://doi.org/10.1175/1520-0442(1999)012<2679:icitem>2.0.co;2

Wan, G. J., Santschi, P. H., Sturm, M., Farrenkothen, K., Lueck, A., Werth, E., & Schuler, C. (1987). Natural ($^{210}$Pb, $^{7}$Be) and fallout ($^{137}$Cs, $^{239,240}$ Pu, $^{90}$Sr) radionuclides as geochemical tracers of sedimentation in Greifensee, Switzerland. *Chemical geology, 63*(3-4), 181-196. https://doi.org/10.1016/0009-2541(87)90162-8

Wang, C., Zhao, Y., Zou, X., Xu, X., & Ge, C. (2017). Recent changing patterns of the Changjiang (Yangtze River) Estuary caused by human activities. *Acta*

*Oceanologica Sinica, 36*(4), 87-96. https://doi.org/10.1007/s13131-017-1017-z

Wang, F., Nian, X., Wang, J., Zhang, W., Peng, G., Ge, C., et al. (2018). Multiple dating approaches applied to the recent sediments in the Yangtze River (Changjiang) subaqueous delta. *Holocene, 28*(6), 858-866. https://doi.org/10.1177/0959683617752847

Wang, T., Zou, X., Li, B., Yao, Y., Zang, Z., Li, Y., et al. (2018). Preliminary study of the source apportionment and diversity of microplastics: Taking floating microplastics in the South China Sea as an example. *Environmental Pollution, 245*, 965-974. https://doi.org/10.1016/j.envpol.2018.10.110

Zhao, Y., Zou, X., Gao, J., Xu, X., Wang, C., Tang, D., et al. (2015). Quantifying the anthropogenic and climatic contributions to changes in water discharge and sediment load into the sea: A case study of the Yangtze River, China. *Science of The Total Environment, 536*, 803-812. https://doi.org/10.1016/j.scitotenv.2015.07.119

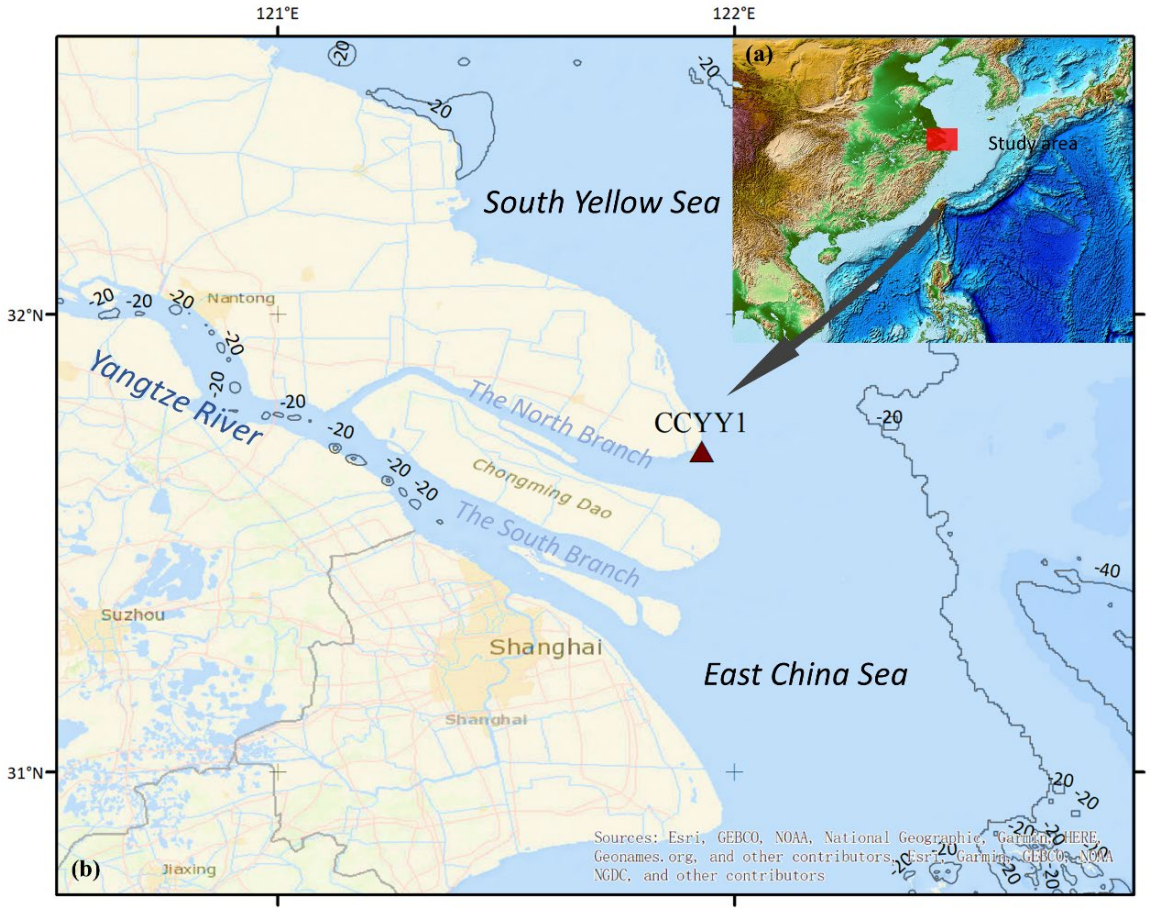


**Figure S1.** Map of the study area. (a) Schematic map of the coastal zone of China, with the Yangtze Estuary marked in red. (b) Yangtze Estuary and the location of CCYY1. The base map is derived from ERIS. The blue lines represent the waterway, the orange lines represent the roads, and urban areas are depicted in yellow.

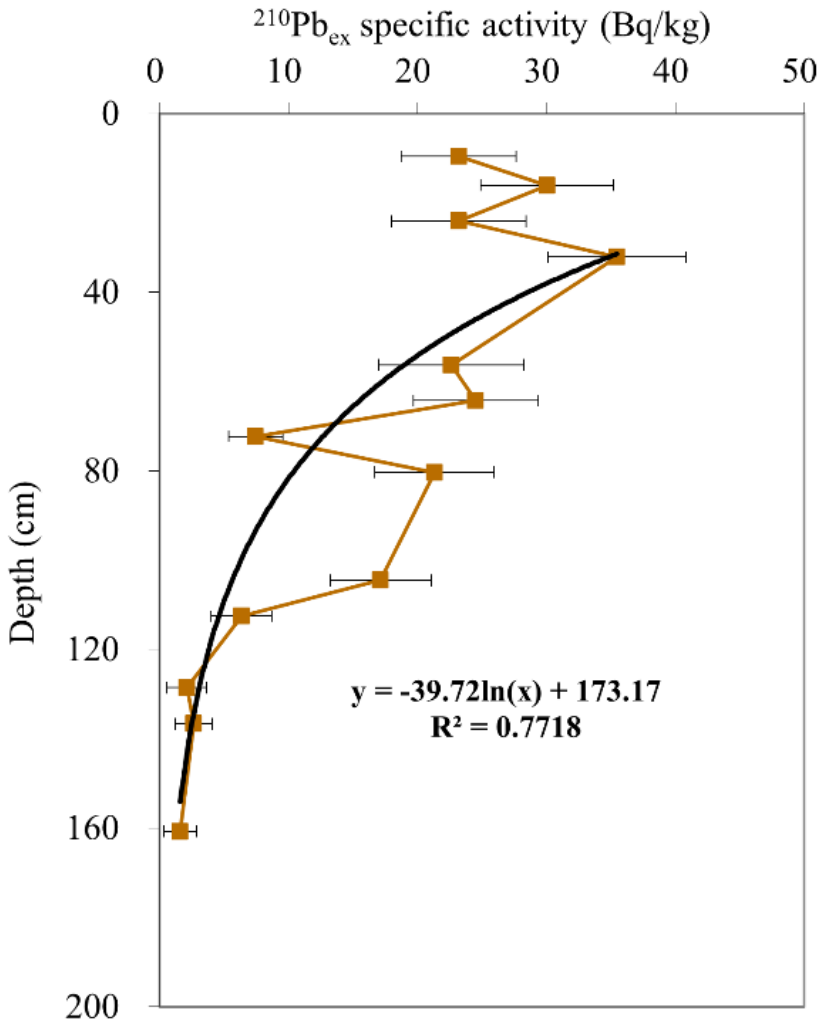


**Figure S2.** Vertical distribution of excess $^{210}$Pb activity of CCYY1

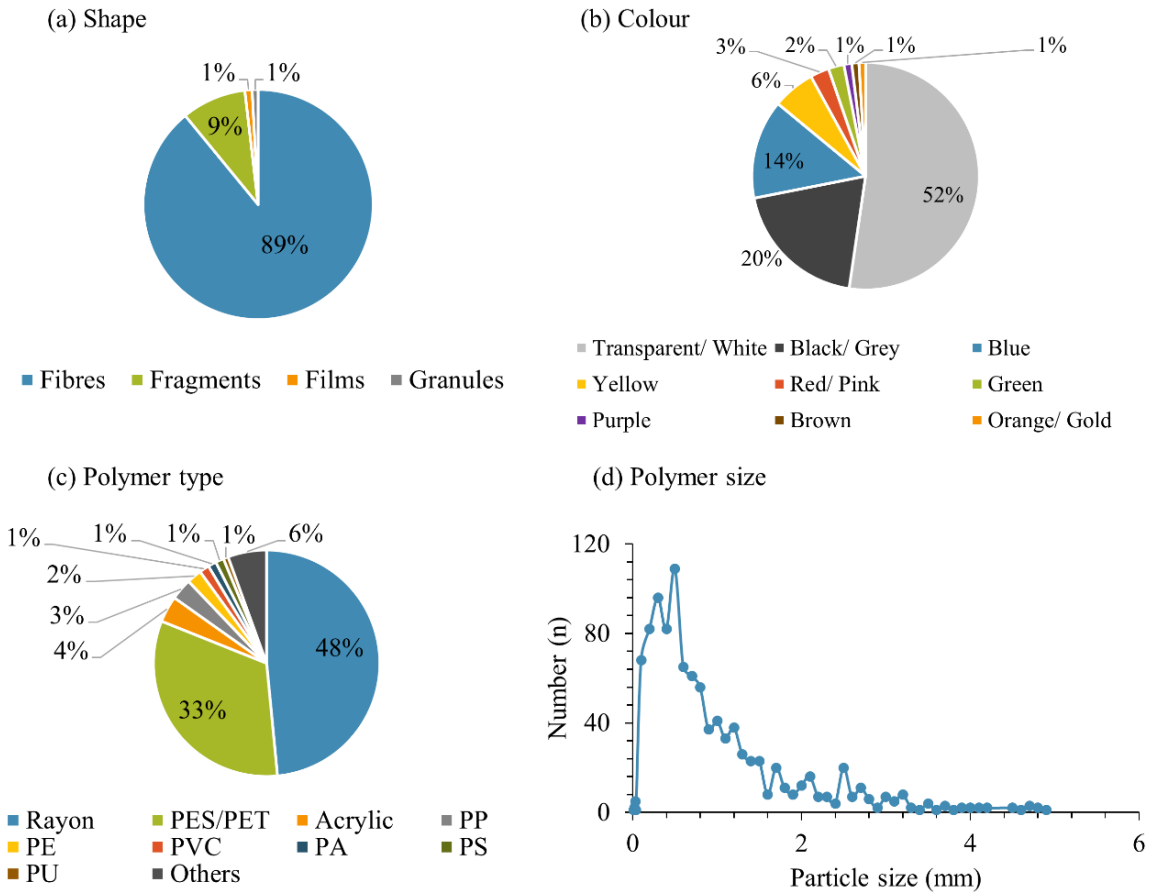


**Figure S3.** Summary of the (a) shape, (b) colour, (c) polymer type and (d) particle size characteristics of microplastics (all layers combined).

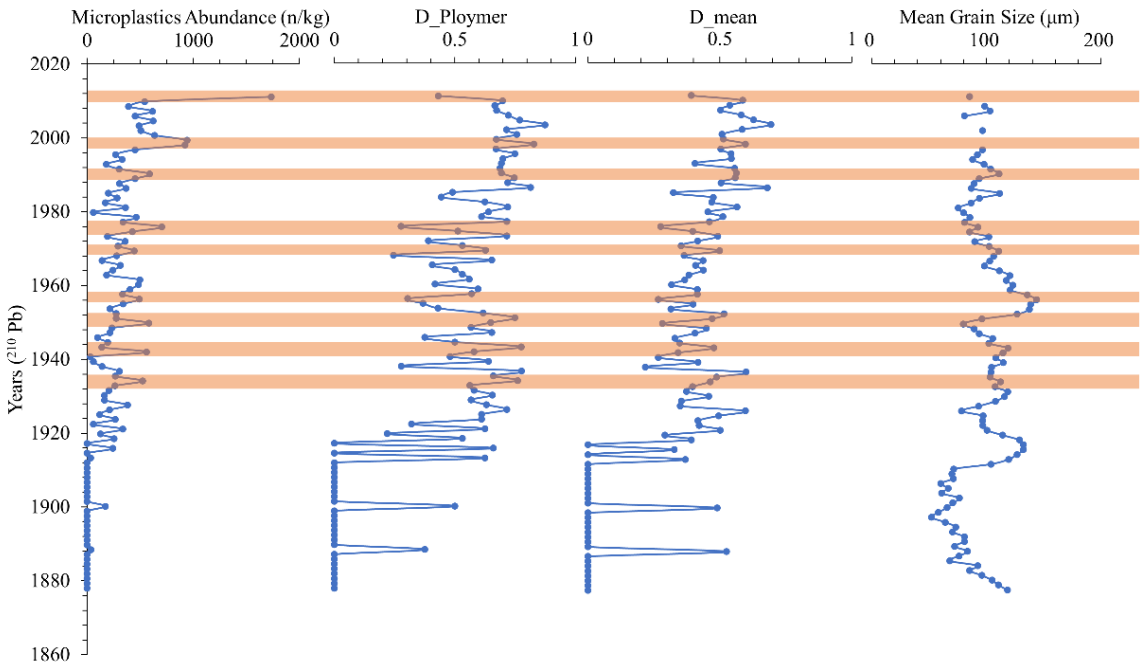


**Figure S4.** Extreme flood events identified by microplastic index (including microplastic abundance, polymer type diversity (D_Ploymer) and mean diversity (D_mean)) and grain size index. Mean diversity is the average of shape diversity, colour diversity and polymer type diversity. Extreme flood events are marked with orange blocks.

| Location | Location type | Microplastic abundance of surface sediment | Reference |
|---|---|---|---|
| South Branch of the Yangtze Estuary | Tidal flat | 3420±1.31 n/kg (dw) | (Zhu et al., 2018) |
| North Branch of the Yangtze Estuary | Tidal flat | 1734.675 n/kg (dw) | This study |
| A cruise along the Yangtze Estuary | River course | 121±9 n/kg (dw) | (Peng et al., 2017) |
| Yangtze Estuary - Hangzhou Bay | River course | Flooding season: 111.2±10.75 n/kg (dw); Dry season: 200±17.3 n/kg (dw) | (Xu et al., 2019) |
| Nanhui tidal flat in the South Branch of the Yangtze Estuary | Tidal flat | 143±0.3 n/kg (dw) | (Wu et al., 2020) |
| South Branch of the Yangtze Estuary | / | ~80 n/kg (dw) | (Su et al., 2018) |
| Chongming Island | Shore of inland river and Yangtze River shore | 10-60 n/kg (dw) | (Y. Li et al., 2020) |

**Table S1.** Comparison of microplastic abundance in surface sediment across the Yangtze Estuary

**Reference**

Li, Y., Lu, Z., Zheng, H., Wang, J., & Chen, C. (2020). Microplastics in surface water and sediments of Chongming Island in the Yangtze Estuary, China. *Environmental Sciences Europe, 32*(15), 1-12. https://doi.org/10.1186/s12302-020-0297-7

Peng, G., Zhu, B., Yang, D., Su, L., Shi, H., & Li, D. (2017). Microplastics in sediments of the Changjiang Estuary, China. *Environmental Pollution, 225*, 283-290.

https://doi.org/10.1016/j.envpol.2016.12.064

Su, L., Cai, H., Kolandhasamy, P., Wu, C., Rochman, C. M., & Shi, H. (2018). Using the Asian clam as an indicator of microplastic pollution in freshwater ecosystems. *Environmental Pollution, 234*, 347-355. https://doi.org/10.1016/j.envpol.2017.11.075

Wu, F., Pennings, S. C., Tong, C., & Xu, Y. (2020). Variation in microplastics composition at small spatial and temporal scales in a tidal flat of the Yangtze Estuary, China. *Science of The Total Environment, 699*, 134252. https://doi.org/10.1016/j.scitotenv.2019.134252

Xu, P., Peng, G. Y., Zhu, L. X., Bai, M. Y., & Li, D. J. (2019). Spatial-temporal distribution and pollution load of microplastics in the Changjiang Estuary. *Zhongguo Huanjing Kexue/China Environmental Science, 39*(5), 2071-2077. https://doi.org/10.19674/j.cnki.issn1000-6923.2019.0248

Zhu, X. T., Yi, J., Qiang, L. Y., & Cheng, J. P. (2018). Distribution and Settlement of Microplastics in the Surface Sediment of Yangtze Estuary. *Huanjing Kexue/Environmental Science, 39*(5), 2067-2074. https://doi.org/10.13227/j.hjkx.201709032

**Data Set S1.** Microplastic properties

**Data Set S2.** Sediment grain size